

# Finite temperature Casimir effect for graphene

Ignat V. Fialkovsky,<sup>1,3,\*</sup> Valery N. Marachevsky,<sup>3,†</sup> and Dmitri V. Vassilevich<sup>2,3,‡</sup>

<sup>1</sup>*Instituto de Física, Universidade de São Paulo,*

*Caixa Postal 66318 CEP 05314-970, São Paulo, S.P., Brazil*

<sup>2</sup>*CMCC, Universidade Federal do ABC, Santo André, S.P., Brazil*

<sup>3</sup>*Department of Theoretical Physics, Saint-Petersburg State University, St. Petersburg 198504, Russia*

We adopt the Dirac model for quasiparticles in graphene and calculate the finite temperature Casimir interaction between a suspended graphene layer and a parallel conducting surface. We find that at high temperature the Casimir interaction in such system is just one half of that for two ideal conductors separated by the same distance. In this limit single graphene layer behaves exactly as a Drude metal. In particular, the contribution of the TE mode is suppressed, while one of the TM mode saturates the ideal metal value. Behavior of the Casimir interaction for intermediate temperatures and separations accessible for an experiment is studied in some detail. We also find an interesting interplay between two fundamental constants of graphene physics: the fine structure constant and the Fermi velocity.

PACS numbers: 12.20.Ds, 73.22.-f

Keywords: graphene, Casimir effect

## I. INTRODUCTION

Nowadays, graphene does not require any long introduction. Its exceptional properties (see reviews [1, 2]) have put graphene in the focus of current research in condensed matter physics and far beyond. The principal feature of graphene is the linear dispersion law  $\omega = v_F k$  ( $v_F = c/300$  is a Fermi velocity,  $c$  is the speed of light in vacuum) for quasi-particle fermion excitations above graphene Fermi surface, which is valid for  $N = 4$  species of fermion excitations in a graphene layer. This law is valid for the energies up to a few eV. The dynamics of quasi-particles and their interaction with electromagnetic field are therefore well described by the quasi-relativistic Dirac model [3]. The propagation of electromagnetic field in the presence of a graphene layer is governed by the effective action where the fermionic excitations are integrated out. To the lowest order this action is determined by the standard polarization operator of 2 + 1 dimensional fermions. Such diagrams have been calculated in a number of papers, see [4–6]. One of the most spectacular predictions of the Dirac model is the universal absorption law for light passing through suspended layers of graphene. This law was experimentally checked with a high precision [7]. There are also other experimental confirmations of the Dirac model, most important of which is the observation of the non-conventional quantum Hall effect, [8].

In this paper we study the Casimir interaction at non-zero temperature of a graphene layer with a parallel metal, using the quasi-relativistic Dirac model for descriptions of quasiparticles in a graphene. In the framework of this model the problem was already addressed in [9], where it was shown that at zero temperature the interaction between graphene and an ideal conductor is about 2.6% of the interaction between two ideal conductors separated by the same distance. Earlier, similar calculations were done [10–12] for the hydrodynamic model, which does not reproduce linear spectrum of low-energy excitations in graphene. More recently, thermal Casimir interaction between graphene layers was calculated in [13] in a van der Waals type approach, i.e. basing on the non-retarded Green's functions. In [14] in the framework of the quasi-relativistic Dirac model it was found that the Casimir interaction between two suspended graphene layers becomes strong at high temperature due to matter plasmonic response in a graphene layer. In another paper, Ref. [15], where graphene was modelled by a combination of Lorentz-type oscillators, practically no temperature dependence of the Casimir force was found.

Temperature dependence of the Casimir interaction attracts much attention due to the unresolved problem of its asymptotics for metals at large separations and finite temperatures [16–21]. Two models of dielectric permittivity, the Drude model and the plasma one, lead to essentially different Casimir interaction due to their different infrared frequency dependence [22–25]. The free energy of two metals with parallel surfaces separated by a vacuum slit  $a$ ,

---

\*Electronic address: ifialk@gmail.com

†Electronic address: maraval@mail.ru

‡Electronic address: dvassil@gmail.com

for  $a \gtrsim \hbar c / (4\pi k_B T)$  is twice as much for the plasma model than for the Drude one [22, 23, 26]. Various theoretical models were used to substantiate arguments in favor of the high temperature behavior characteristic for a Drude model [27–30]. Predictions of the models also differ at shorter separations where most experiments are being performed. However, a discussion of whether one of the models is excluded by existing experimental data is still under way [31, 32]. At the same time, we would like to emphasize that the main predictions of the paper are insensitive to particular model used for description of conductivity of metal (see discussion in Section IV.A).

The results of the paper are outlined below in brief. In Section II we derive a polarization operator for 2+1 Dirac fermions at finite temperature and chemical potential. It allows us to describe in Sect. III optical properties of graphene in terms of the components of polarization operator using the modified Maxwell equations for classical electromagnetic field in the presence of a suspended graphene layer. Basing on this, we perform in Section IV a detailed study of the Lifshitz free energy of a graphene layer interacting with a parallel metal. In Sect. IV.A we derive the high temperature asymptotics of the free energy of the system, which appears to be the same as for two conducting surfaces described by the Drude model, i.e. surprisingly strong for a monoatomic graphene layer. In Sect. IV.B we investigate in detail the contribution of non-zero Matsubara terms, and discuss different scaling regimes of the free energy specific to considered graphene-metal system. In Conclusions we outline our main results.

In what follows we adopt  $\hbar = c = k_B = 1$ .

## II. THE DIRAC MODEL

The dynamics of quasi-particles in graphene is well described within a 2 + 1-dimensional Dirac model. All the most important properties of low-energy excitations are indeed readily incorporated in this model: the linearity of the spectrum at the energies below approximately 1eV, a very small mass gap (if any, but see discussion in [4–6, 33]), and the different “speed of light” inside the graphene layer  $v_F \simeq (300)^{-1}$ . Moreover, the interaction of the quasi-particles with either quantum or classical external electromagnetic field is straightforwardly described within this model by a standard “covariantization” of the derivative with help of electromagnetic potential  $A_\mu$ . Thus one deals with the model described by the following classical action (assuming graphene plane lying at  $x^3 = 0$ )

$$S = -\frac{1}{4} \int d^4x F_{\mu\nu}^2 + \int d^3x \bar{\psi} \not{D} \psi \quad (1)$$

with

$$\not{D} = (i\partial_0 - \mu - eA_0)\gamma_0 + v_F[\gamma^1(i\partial_1 - eA_1) + \gamma^2(i\partial_2 - eA_2)] - m.$$

Since there are  $N = 4$  species of fermions in graphene, the gamma matrices are in fact  $8 \times 8$ , being a direct sum of four  $2 \times 2$  representations (with two copies of each of the two inequivalent ones),  $\gamma_0^2 = -(\gamma^{1,2})^2 = 1$ . The Maxwell action is normalized in such a way that

$$e^2 \equiv 4\pi\alpha = \frac{4\pi}{137}. \quad (2)$$

The properties of the electromagnetic field (both classical, and quantum) in presence of a single graphene layer can be deduced from the partition function

$$Z = \int D[A\bar{\psi}\psi] e^{iS}.$$

where  $S$  is given by (1). Depending on the problem under consideration we can also constrain the electromagnetic potential  $A$  with some additional conditions. In particular, investigating the Casimir interaction between graphene and parallel ideal conductor we will impose the conductor boundary conditions at  $x^3 = a$

$$A_0|_{x^3=a} = A_1|_{x^3=a} = A_2|_{x^3=a} = \partial_3 A_3|_{x^3=a} = 0. \quad (3)$$

thus making the partition function dependent on the distance between graphene and the metal,  $Z \equiv Z(a)$ .

As the first step of consideration, one shall integrate out fermions thus obtaining

$$Z = \int DA e^{-\frac{i}{4} \int d^4x F_{\mu\nu}^2 + iS_{\text{eff}}(A)} \quad (4)$$

At a somewhat formal level

$$S_{\text{eff}}(A) \equiv -i \ln \det(\not{D}). \quad (5)$$

Since the action (1) is quadratic in  $\psi$ , the expression (4) is exact, though one has to give a precise meaning to the determinant (5).

In the quadratic approximation the effective action  $S_{\text{eff}}(A)$  discussed above reads

$$S_{\text{eff}}(A) = A \text{---} \text{---} \text{---} A = \frac{1}{2} \int \frac{d^3 p}{(2\pi)^3} A_j(p) \Pi^{jl}(p) A_l(p), \quad (6)$$

The polarization operator  $\Pi_{ij}$  has been considered in a number of papers for the systems characterized by various sets of parameters. For the zero-temperature case it has been first calculated in [4], for non-zero  $T$  in [34], other cases were considered in, e.g., [6, 35]. Here we present the general result for  $\Pi_{ij}(p_0, \mathbf{p})$  depending on non-vanishing  $m, \mu, T$ . The final formulae (9), (13) coincide with the cases presented in the literature provided one considers appropriate limits of parameters. In particular, (A.27) of [34] can be obtained from our result (13) for  $m = \mu = 0$  and  $v_F = 1$ , while (30) of [35] in the case of  $\Gamma = 0$  is equal to (13) in the limit  $p_0 \rightarrow 0$ . The calculations are therefore quite standard though tedious. We shall be rather sketchy in their description.

In Minkowski space the one-loop polarization operator can be expressed in momentum space as

$$\Pi^{mn}(p_0, \mathbf{p}) = ie^2 \int \frac{dq_0 d^2 \mathbf{q}}{(2\pi)^3} \text{tr} \left( \hat{S}(q_0, \mathbf{q}) \tilde{\gamma}^m \hat{S}(q_0 - p_0, \mathbf{q} - \mathbf{p}) \tilde{\gamma}^n \right), \quad (7)$$

where the propagator of the quasiparticles in graphene reads

$$\hat{S}(q_0, \mathbf{q}) \equiv \mathcal{D}^{-1}|_{A_\mu=0} = -\frac{(q_0 + \mu)\gamma_0 - v_F \boldsymbol{\gamma} - m}{(q_0 + \mu + i\epsilon \text{sgn} q_0)^2 - v_F^2 \mathbf{q}^2 - m^2}. \quad (8)$$

Note that due to the quasi-relativistic nature of excitations in graphene  $\hat{S}$  also depends on the Fermi velocity  $v_F$ . Here  $\mathbf{q}^j = (q^1, q^2)$ ,  $\boldsymbol{\gamma} = \gamma^1 q_1 + \gamma^2 q_2$ .

Due to the Lorenz and gauge invariance (transversality) the polarization tensor in an empty space can be completely defined by calculating a single scalar function. In the presence of medium characterized by the velocity  $u$  one needs two independent components for complete definition of the (parity-even)  $\Pi^{ij}$  [36]

$$\Pi^{mn} = \frac{1}{v_F^2} \eta_j^m \left[ \Pi_0^{ji} A(p_0, \mathbf{p}) + p_0^2 \Pi_u^{ji} B(p_0, \mathbf{p}) \right] \eta_i^n \quad (9)$$

$$\Pi_0^{ji} = g^{ji} - \frac{\tilde{p}^j \tilde{p}^i}{\tilde{p}^2}, \quad \Pi_u^{ji} = \frac{\tilde{p}^j \tilde{p}^i}{\tilde{p}^2} - \frac{\tilde{p}^j u^i + u^j \tilde{p}^i}{(\tilde{p}u)} + \frac{u^j u^i}{(\tilde{p}u)^2 \tilde{p}^2}$$

where  $\eta = \text{diag}(1, v_F, v_F)$ , and  $A, B$  are scalar functions. Note, that in this expression we also took into account the above mentioned quasi-relativistic nature of the excitation in graphene by introducing an appropriate dependence on  $v_F$ . Vectors with tilde are rescaled by multiplying the spatial components with  $v_F$ , i.e.,  $\tilde{p}^j \equiv \eta_i^j p^i = (p_0, v_F \mathbf{p})$ . For more details see, e.g., [37].

In the medium rest reference frame,  $u = (1, 0, 0)$ , the scalar functions  $A, B$  can be expressed via the temporal component of the polarization operator and its trace in the following way ( $p_3^2 \equiv p_0^2 - \mathbf{p}^2$ ,  $\tilde{p}_3^2 \equiv p_0^2 - v_F^2 \mathbf{p}^2$ )

$$A = \frac{p_3^2}{\mathbf{p}^2} \Pi_{00} + \Pi_{\text{tr}}, \quad B = \frac{1}{v_F^2 \mathbf{p}^2} \left( \frac{p_3^2 + \tilde{p}_3^2}{\mathbf{p}^2} \Pi_{00} + \Pi_{\text{tr}} \right). \quad (10)$$

Clearly, we can express  $A, B$  through any pair of the components of  $\Pi$ . We choose  $\Pi_{\text{tr}} \equiv \Pi_m^m$  and  $\Pi_{00}$  for convenience of further calculations. In what follows we sketch the derivation of the temporal component  $\Pi_{00}$  only, while the trace is calculated similarly.

To introduce the temperature in (7) we perform the rotation to the Matsubara frequencies (see, e.g. [38])

$$i \int dq_0 \rightarrow -2\pi T \sum_{k=-\infty}^{\infty}, \quad q_0 \rightarrow 2\pi i T(k + 1/2), \quad (11)$$

use the Feynman parametrization

$$\frac{1}{ab} = \int_0^1 \frac{dx}{(xa + (1-x)b)^2}$$

and subsequently change the variables in (7) in the spatial part of the loop-integration:  $\mathbf{q} \rightarrow \mathbf{q} + x\mathbf{p}$ . Then we come to

$$\Pi^{00} = -2e^2TN \sum_{k=-\infty}^{\infty} \int_0^1 dx \int \frac{d^2\mathbf{q}}{(2\pi)^2} \frac{M_0^2 - (q_0 + \mu)(p_0 - q_0 - \mu)}{[(q_0 + \mu - xp_0)^2 - \Theta^2]^2}$$

with  $M_0^2 = m^2 + v_F^2\mathbf{q}^2 - x(1-x)v_F^2\mathbf{p}^2$  and

$$\Theta^2 = m^2 + v_F^2\mathbf{q}^2 - x(1-x)(p_0^2 - v_F^2\mathbf{p}^2).$$

Summation over the fermion Matsubara frequencies can be made explicitly

$$\sum_{k=-\infty}^{\infty} \frac{1}{[(2\pi iT(k+1/2) - b)^2 - \Theta^2]^2} = -\frac{1}{16\Theta^3 T^2} \left( \Theta \operatorname{sech}^2 \left( \frac{\Theta + b}{2T} \right) - 2T \tanh \left( \frac{\Theta + b}{2T} \right) \right) + (\Theta \rightarrow -\Theta). \quad (12)$$

The  $\mathbf{q}$ -integration can also be performed directly by using that  $\partial_x \tanh x = \operatorname{sech}^2 x$ . After these transformations only the integral over  $x$  remains, and we arrive at the following representation for  $\Pi_{00}$  and  $\Pi_{\text{tr}}$

$$\Pi_{\text{tr},00} = -\frac{2N\alpha T}{v_F^2} \int_0^1 dx \left( f_{\text{tr},00} \tanh \frac{\Theta_0 + b}{2T} - \ln \left( 2 \cosh \frac{\Theta_0 + b}{2T} \right) \right) + (\Theta_0 \rightarrow -\Theta_0) \quad (13)$$

where  $\Theta_0 \equiv \sqrt{m^2 - x(1-x)(p_0^2 - v_F^2\mathbf{p}^2)}$ ,  $b = p_0x - \mu$ , and

$$f_{00} = \frac{-2v_F^2\mathbf{p}^2x(1-x) - p_0(1-2x)\Theta_0 + 2\Theta_0^2}{4T\Theta_0}. \quad (14)$$

$$f_{\text{tr}} = \frac{2m^2v_F^2 + 2x(1-x)v_F^2p_3^2}{4T\Theta_0} - \frac{p_0(1-2v_F^2)(1-2x) - 2(1-v_F^2)\Theta_0}{4T}. \quad (15)$$

We remind that  $N$  is the number of fermion species,  $N = 4$  for graphene. Parity-odd contributions to the polarization tensor cancel out between different species, while the parity-even contributions add up.

We note here that the expression (7) is power-counting divergent. An ultra-violet divergence indeed appears in the trace part  $\Pi_m^m$ . To remove this divergence we performed the Pauli-Villars subtraction at an infinite mass, which is a rather standard procedure. One can check that the  $m \rightarrow \infty$  limit of (13) is indeed zero.

### III. REFLECTION COEFFICIENTS

In our approximation the full action for the electromagnetic field is  $-\frac{1}{4} \int d^4x F_{\mu\nu}^2 + S_{\text{eff}}$ , where the effective action (6) is confined to the surface of graphene, which we place at  $x^3 = 0$ . This action is singular and gives rise to an interaction proportional to  $\delta(x^3)$  and depending on the tangential momenta. Therefore, the Maxwell equations receive a singular contribution

$$\partial_\mu F^{\mu\nu} + \delta(x^3)\Pi^{\nu\rho}A_\rho = 0. \quad (16)$$

We extended  $\Pi$  to a  $4 \times 4$  matrix with  $\Pi^{3\mu} = \Pi^{\mu 3} = 0$ . The equations (16) describe a free propagation of the electromagnetic field outside the surface  $x^3 = 0$  subject to the matching conditions

$$\begin{aligned} A_\mu|_{x^3=+0} &= A_\mu|_{x^3=-0}, \\ (\partial_3 A_\mu)|_{x^3=+0} - (\partial_3 A_\mu)|_{x^3=-0} &= \Pi_\mu^\nu A_\nu|_{x^3=0} \end{aligned} \quad (17)$$

on that surface. So far, the only difference from the zero-temperature case [9] is in the form of  $\Pi_\nu^\mu$ . These matching conditions can also be rewritten in terms of the electric and magnetic fields  $\mathbf{E}$ ,  $\mathbf{H}$ .

Next, we introduce a TE mode

$$\mathbf{E} = (-p_2\mathbf{e}_1 + p_1\mathbf{e}_2)p_0\Psi(x^3) \quad (18)$$

$$\mathbf{H} = i(p_1\mathbf{e}_1 + p_2\mathbf{e}_2)\Psi'(x^3) + \mathbf{e}_3(p_1^2 + p_2^2)\Psi(x^3) \quad (19)$$

$$(20)$$

and a TM mode

$$\mathbf{E} = i(p_1\mathbf{e}_1 + p_2\mathbf{e}_2)\Phi'(x^3) + \mathbf{e}_3(p_1^2 + p_2^2)\Phi(x^3) \quad (21)$$

$$\mathbf{H} = (p_2\mathbf{e}_1 - p_1\mathbf{e}_2)p_0\Phi(x^3) \quad (22)$$

$$(23)$$

where  $\mathbf{e}_1, \mathbf{e}_2, \mathbf{e}_3$  are unit vectors. An overall factor of  $\exp(i(x^0p_0 + x^1p_1 + x^2p_2))$  has been omitted for brevity.

To define the scattering data in the TE and TM sectors we take the potentials in the form

$$\Psi(x^3) = \begin{cases} e^{ip_3x^3} + r_{\text{TE}}e^{-ip_3x^3}, & x^3 < 0 \\ t_{\text{TE}}e^{ip_3x^3}, & x^3 > 0 \end{cases}, \quad \Phi(x^3) = \begin{cases} e^{ip_3x^3} + r_{\text{TM}}e^{-ip_3x^3}, & x^3 < 0 \\ t_{\text{TM}}e^{ip_3x^3}, & x^3 > 0 \end{cases} \quad (24)$$

The reflection and transmission coefficients are defined by the matching conditions. After some algebra we obtain

$$r_{\text{TE}} = \frac{A}{2ip_3 - A}, \quad t_{\text{TE}} = \frac{2ip_3}{2ip_3 - A} \quad (25)$$

$$r_{\text{TM}} = -\frac{p_3(A - v_F^2\mathbf{p}^2B)}{2i\tilde{p}_3^2 - p_3(A - v_F^2\mathbf{p}^2B)}, \quad t_{\text{TM}} = \frac{2i\tilde{p}_3^2}{2i\tilde{p}_3^2 - p_3(A - v_F^2\mathbf{p}^2B)}.$$

For the later use in the Lifshitz formula (27) for the Casimir energy, one can also rewrite the reflection coefficients in terms of the polarization tensor components

$$r_{\text{TM}} = \frac{p_3\Pi_{00}}{p_3\Pi_{00} + 2i\mathbf{p}^2}, \quad r_{\text{TE}} = -\frac{p_3^2\Pi_{00} + \mathbf{p}^2\Pi_{\text{tr}}}{p_3^2\Pi_{00} + \mathbf{p}^2(\Pi_{\text{tr}} - 2ip_3)}. \quad (26)$$

The predictions of (26) for the visible light appear to be essentially the same as for the idealized ( $m = \mu = 0$ ) zero-temperature case [37] since the corresponding frequencies are much higher than any other scales in a realistic graphene sample.

We stress that here we are working with free standing samples of graphene. Otherwise, the substrate will contribute to the reflection coefficients.

#### IV. FREE ENERGY

As early as in 1955 Lifshitz demonstrated [39] that the Casimir interaction between two parallel dielectric slabs can be expressed in a closed form if their dielectric permittivities are known at the imaginary frequencies. In a number of later works the original calculation was generalized and refined [40–43]. In particular, it was shown by Kats [40] that for any two given parallel plane interfaces separated by the distance  $a$  and described by their reflection coefficients  $r_{\text{TE,TM}}^{(1)}, r_{\text{TE,TM}}^{(2)}$  of the TE and TM electromagnetic modes, the Lifshitz free energy density reads

$$\mathcal{F} = T \sum_{n=-\infty}^{\infty} \int \frac{d^2\mathbf{p}}{8\pi^2} \ln[(1 - e^{-2p_{\parallel}a}r_{\text{TE}}^{(1)}r_{\text{TE}}^{(2)})(1 - e^{-2p_{\parallel}a}r_{\text{TM}}^{(1)}r_{\text{TM}}^{(2)})]. \quad (27)$$

where  $p_{\parallel} = \sqrt{\omega_n^2 + \mathbf{p}^2}$ , and  $\omega_n = 2\pi nT$  are the Matsubara frequencies. The reflection coefficients here are assumed to be also taken at Euclidian momenta  $r = r(\omega_n, \mathbf{p})$ .

Choosing as interacting interfaces a suspended graphene film and a parallel ideal metal, we shall substitute in the above the corresponding reflection coefficients. For the perfect conductor one has

$$r_{\text{TM}}^{(2)} = 1, \quad r_{\text{TE}}^{(2)} = -1. \quad (28)$$

The reflection coefficients for graphene at Euclidian momenta can be found after the substitution  $p_0 = i2\pi nT = i\omega_n$  into the formulas (13-15),(26). More precisely, in (26), one should replace  $p_3$  by  $i\sqrt{\omega_n^2 + \mathbf{p}^2}$ .

In the following section V.A we consider the high temperature (large separation) asymptotics of the graphene-ideal metal free energy, while in subsequent section V.B we study the case  $m = \mu = 0$  analytically and discuss numerical results.

### A. High temperature limit

As discussed in the introduction, the high temperature limit is the most intriguing regime in the Casimir physics. In this limit at distances  $H \equiv 4\pi aT \gg 1$ , the zero frequency Matsubara terms determine the free energy since other Matsubara terms are exponentially suppressed at these separations. As we show below, at zero frequency  $r_{\text{TM}} \sim 1$ ,  $r_{\text{TE}} \sim \alpha N v_F^2 |\mathbf{p}|$  for small values of the wave vector  $|\mathbf{p}|$ . Thus the coefficient  $r_{\text{TM}}$  acquires the ideal metal value, and this is the principal feature of graphene at high temperatures. At the same time, the TE mode free energy for graphene-metal is suppressed at separations  $a \gtrsim 1/(4\pi T)$  by a factor  $\alpha N v_F^2 / (aT) \ll 1$ , and due to this suppression the difference in this regime in the results for the ideal metal and the Drude or the plasma models of a real metal is too small to be observed in possible experiments in graphene-metal system. For other distinctions of the graphene-metal high-temperature asymptotics see the next subsection.

As already mentioned the main contribution in the sum in (27) at high  $aT$  is given by the zero frequency Matsubara term

$$\mathcal{F}_0 = \frac{T^3}{4\pi} \int_0^\infty s ds \ln(1 + r_{\text{TE}} e^{-2aTs}) (1 - r_{\text{TM}} e^{-2aTs}) \quad (29)$$

where we also performed angular integration and re-scaled the momentum,  $s = |\mathbf{p}|/T$  as compared with (27). Further expansion in powers of  $aT$  is determined by the  $s \rightarrow 0$  behavior of the integrand in (29). To obtain corresponding asymptotics we first note that the polarization tensor components at  $\omega_n = 0$  behave as

$$\Pi_{00} \underset{s \rightarrow 0}{\simeq} \frac{2NT\alpha}{v_F^2} \left( \ln \left( 2 \cosh \frac{m + \mu}{2T} \right) - \frac{m}{2T} \tanh \frac{m + \mu}{2T} + (\mu \rightarrow -\mu) \right) + \quad (30)$$

$$+ \frac{\alpha NT^2 s^2}{24m} \left( 2 \tanh \frac{m + \mu}{2T} + \frac{m}{2T} \tanh^2 \frac{m + \mu}{2T} - m + (\mu \rightarrow -\mu) \right) + O(s^4)$$

$$\Pi_{\text{tr}} - \Pi_{00} \underset{s \rightarrow 0}{\simeq} \frac{\alpha NT^2 v_F^2 s^2}{12m} \left( \tanh \frac{m + \mu}{2T} + (\mu \rightarrow -\mu) \right) + O(s^4) \quad (31)$$

From this we readily deduce that

$$r_{\text{TE}} \underset{s \rightarrow 0}{\simeq} - \frac{\alpha NT v_F^2 s}{6m} \left( \tanh \frac{m + \mu}{2T} + (\mu \rightarrow -\mu) \right) + O(s^2), \quad (32)$$

$$r_{\text{TM}} \underset{s \rightarrow 0}{\simeq} 1 - \frac{sv_F^2 / (\alpha N)}{\ln \left( 2 \cosh \frac{m + \mu}{2T} \right) - \frac{m}{2T} \tanh \frac{m + \mu}{2T} + (\mu \rightarrow -\mu)} + O(s^2). \quad (33)$$

where we assumed that  $m$  and  $\mu$  are of the order of the temperature  $T$ , which can be relevant for some particular graphene samples and/or experimental setups. Note that all formulas in this section are also valid for  $m, \mu \rightarrow 0$ , since  $s \rightarrow 0$  is essentially the same limit as  $T \rightarrow \infty$ .

As we can see,  $r_{\text{TE}}$  remains small for the relevant values of momenta. Taking the leading term in the expansion of the logarithm in (29) and using (32) we obtain the leading TE contribution at large separations corresponding to the zero frequency term

$$\mathcal{F}_{0\text{TE}} \simeq - \frac{\alpha NT v_F^2}{192\pi m a^3} \left( \tanh \frac{m + \mu}{2T} + (\mu \rightarrow -\mu) \right). \quad (34)$$

For the TM mode one cannot use the expansion of  $\ln(1 - r_{\text{TM}} e^{-2aTs})$  as it is divergent near  $s = 0$ , see (33). Instead one has to use the representation

$$\mathcal{F}_{0\text{TM}} = \frac{T^3}{4\pi} \int_0^\infty s ds \left( \ln(1 - e^{-2aTs}) + \ln \left( 1 - \frac{r_{\text{TM}} - 1}{1 - e^{-2aTs}} e^{-2aTs} \right) \right). \quad (35)$$

The integral of the first term can be taken explicitly leading to

$$\mathcal{F}_{0\text{TM}}^{(0)} = - \frac{k_B T \zeta(3)}{16\pi a^2} \equiv \mathcal{F}_{\text{Drude}}|_{T \rightarrow \infty} = \frac{1}{2} \mathcal{F}_{\text{id}}|_{T \rightarrow \infty}, \quad (36)$$

which coincides exactly with the interaction of two real metals at high temperature described by the Drude model, or, equivalently, one half of interaction between two ideal metals at high temperature,  $\mathcal{F}_{\text{id}}$ . For readability, in (36) we temporarily restored the physical units. In the rest of (35) one can use an expansion

$$\mathcal{F}_{0\text{TM}}^{(1)} = -\frac{T^3}{4\pi} \sum_{l=1}^{\infty} \frac{1}{l} \int_0^{\infty} s ds \left( \frac{r_{\text{TM}} - 1}{1 - e^{-2aTs}} \right)^l e^{-2laTs}. \quad (37)$$

As the main contribution to the asymptotics at  $H \rightarrow \infty$  comes from vicinity of  $s = 0$  we can expand  $r_{\text{TM}} - 1$  in a Taylor series around this point, to obtain in the highest order

$$\begin{aligned} \mathcal{F}_{0\text{TM}}^{(1)} &\simeq -\frac{T^3}{4\pi} \sum_{l=1}^{\infty} \frac{\left(r_{\text{TM}}^{(1)}\right)^l}{l} \int_0^{\infty} s^{l+1} (1 + O(s)) \left( \frac{e^{-2aTs}}{1 - e^{-2aTs}} \right)^l ds \\ &= -\frac{T^3}{4\pi} \sum_{l=1}^{\infty} \frac{1}{l} \frac{\left(r_{\text{TM}}^{(1)}\right)^l C_l}{(2aT)^{l+2}} \left( 1 + O\left(\frac{1}{2aT}\right) \right) \simeq -\frac{T^3}{4\pi} \frac{r_{\text{TM}}^{(1)} C_1}{(2aT)^3} = -\frac{\zeta(3) r_{\text{TM}}^{(1)}}{16\pi a^3} \end{aligned} \quad (38)$$

where  $C_l = \int_0^{\infty} s^{l+1} \left( \frac{e^{-s}}{1 - e^{-s}} \right)^l ds$  and  $r_{\text{TM}}^{(1)} \equiv \left( \frac{\partial}{\partial s} r_{\text{TM}} \right)_{s=0}$  which can be deduced from (33). In graphene, where  $v_F^2/(\alpha N) \ll 1$ , this correction is already small for considered  $H = 4\pi aT \gtrsim 1$ , but in other Dirac systems with larger  $v_F$ , the transition of  $\mathcal{F}_{0\text{TM}}$  (35) to asymptotic (36) would occur only at much higher distances  $aT \gg v_F^2/(\alpha N)$ . We call attention of the reader that in any case this condition does not define the transition to the high-temperature regime of the whole free energy (27) which also includes the nonzero Matsubara terms. In the next subsection we investigate in detail their contribution and define through a scaling argument the transition condition for graphene-metal system as  $aT \gg \alpha \ln \alpha^{-1}/(2\zeta(3)) \simeq 0.015$ .

Thus we can say, that from (34), (36) and (38), and considerations of the next subsection it follows that for separations  $H \gg 0.19$  the main contribution to the interaction of a suspended graphene layer with ideal conductor comes from the TM mode leading contribution (36) and asymptotically constitutes just one half of the interaction between two ideal metals at large separations. This is induced by the specific dependence of the TE,M reflection coefficients on the momenta  $s = |\mathbf{p}|/T$  for small  $s$ , see (32),(33). As mentioned earlier, such  $r_{\text{TM,E}}$  behavior also makes the predictions for large separations insensitive to the differences between Drude and plasma models of conductivity of a real metal in possible experiments. A numerical analysis shows that the difference between graphene-ideal metal and graphene-gold free energies becomes small already at  $a \gtrsim 100\text{nm}$  at  $T = 300\text{K}$  (see Fig.2) and rapidly decreases with higher separations. Moreover, in this limit the interaction of two suspended graphene samples will acquire exactly the same asymptotical value.

As was shown in [9], in the zero-temperature limit the Casimir force between graphene and perfectly conducting metal is about 2.6% of the force between two perfectly conducting metals. As we see, in the opposite limit,  $H \gg 0.19$ , the ratio of graphene - ideal metal free energy to the ideal metal - ideal metal free energy is strongly enhanced. Such an enhancement takes place due to the non-perturbative structure of the Lifshitz result in the limit  $v_F = 0$ .

## B. Further analysis and numerical results

Given the specific values of  $m$  and  $\mu$ , the Casimir interaction can be evaluated by making use of the Lifshitz formula, reflection coefficients and the polarization operator. As our numerical analysis shows, increasing the mass gap diminishes the Casimir interaction (see also a corresponding discussion in [9]), while inclusion of a nonzero chemical potential  $\mu$  enhances the interaction. However, the difference in the values of the free energy for  $m, \mu \sim 0.01\text{eV}$ , which are reasonable bounds for these quantities in suspended graphene samples, and the  $m = \mu = 0$  case is less than one percent. Therefore in what follows we turn our attention to the important case  $m = \mu = 0$  and study it in detail.

It is often desirable to have an accurate analytical approximation of the exact result at different separations. We present such an expression for the sum of nonzero Matsubara terms in this section.

To obtain an appropriate analytical expression we first note that at separations  $H \gg v_F$  one can put  $v_F = 0$  in any nonzero Matsubara term. It is possible due to the exponential factor in the Lifshitz formula which effectively restrains the integration over impulse to  $ap_{\parallel} \lesssim 1$ . In this case contribution of the type of  $v_F^2 (ap_{\parallel})^2$  can be neglected compared to  $(ap_0)^2 = (2\pi naT)^2$  due to the smallness of the parameter  $v_F$ . However, our numerical analysis shows, that this approximation works at smaller distances as well, see below discussion around (46).

Secondly, in the finite temperature sum of nonzero Matsubara terms in the Lifshitz formula one can use the reflection coefficients taken at zero (!) temperature. The corrections due to finite temperature are suppressed for

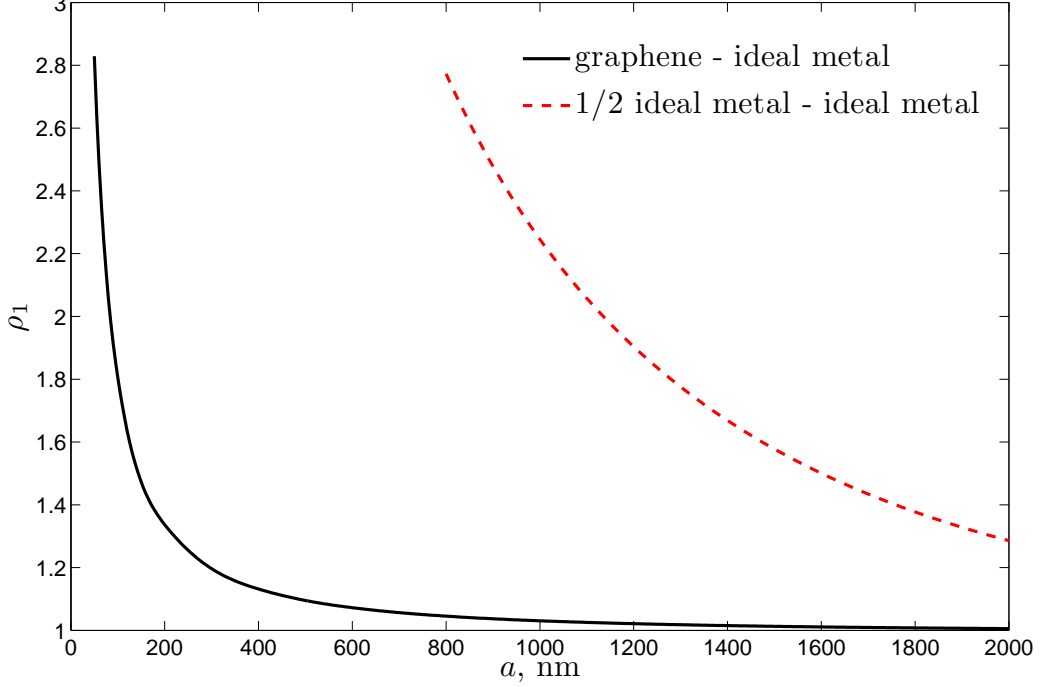


FIG. 1: Ratio  $\rho_1$  of the free energy to the high-temperature asymptotics  $\mathcal{F}_{0\text{TM}}^{(0)}$ , see Eq. (36). Both graphs are calculated for  $T = 300\text{K}$ . In graphene the values  $m = \mu = 0$  were used.

nonzero Matsubara terms, so we neglect them in the leading approximation. Contrary to this, in zero frequency Matsubara terms one has to take into account the whole structure of the finite temperature polarization operator entering  $r_{TE,M}$ .

Under two mentioned above approximations and the condition  $m = \mu = 0$  the reflection coefficients of a single graphene layer at zero temperature have the form:

$$r_{\text{TM}}^{T=0} = \frac{\pi\alpha N \sqrt{p_0^2 + p_{\parallel}^2}}{\pi\alpha N \sqrt{p_0^2 + p_{\parallel}^2} + 8\sqrt{p_0^2 + v_F^2 p_{\parallel}^2}} \simeq \frac{\pi\alpha N \sqrt{p_0^2 + p_{\parallel}^2}}{\pi\alpha N \sqrt{p_0^2 + p_{\parallel}^2} + 8|p_0|} \quad (39)$$

$$r_{\text{TE}}^{T=0} = -\frac{\pi\alpha N \sqrt{p_0^2 + v_F^2 p_{\parallel}^2}}{\pi\alpha N \sqrt{p_0^2 + v_F^2 p_{\parallel}^2} + 8\sqrt{p_0^2 + p_{\parallel}^2}} \simeq -\frac{\pi\alpha N |p_0|}{\pi\alpha N |p_0| + 8\sqrt{p_0^2 + p_{\parallel}^2}} \quad (40)$$

Due to smallness of the reflection coefficients (both being of the order of  $\alpha$ ) we can take just the first term in the expansion of the logarithm in the Lifshitz formula as another reasonable approximation for nonzero Matsubara terms. Note, however, that expansion of the reflection coefficients themselves (at least in TM mode) is not legitimate, as will become evident below.

The sum of nonzero Matsubara terms in this approximation in the TM case with  $r_{\text{TM}}^{(1)} = r_{\text{TM}}^{T=0}$  (39) and  $r_{\text{TM}}^{(2)} = 1$  equals to

$$\begin{aligned} \Delta\mathcal{F}_{\text{TM}} &= -\frac{T}{2\pi} \sum_{n=1}^{+\infty} \int_{Hn/2}^{+\infty} ds_1 \frac{s_1^2}{s_1 + 16nT/(\alpha N)} \exp(-2as_1) = \\ &= -\frac{T}{8\pi a^2} \sum_{n=1}^{+\infty} \exp(-Hn)(1 - gn + Hn) + (gn)^2 \exp(gn)E_1(gn + Hn), \end{aligned} \quad (41)$$

here  $s_1 = \sqrt{\omega_n^2 + p_{\parallel}^2}$  and  $g \equiv 32Ta/(\alpha N)$ ,  $E_1$  stands for the standard exponential integral function. It is convenient to reexpress the result (41) in an integral form. For this purpose one has to differentiate (41) over  $H$ , assuming  $H$  as



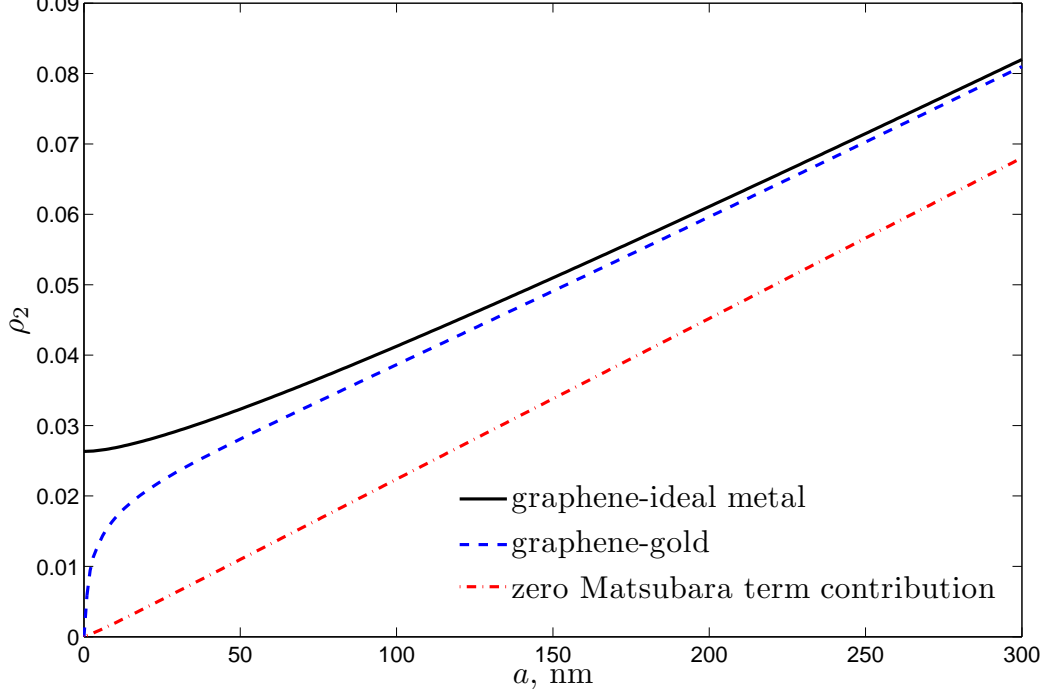


FIG. 2: Ratio  $\rho_2$  of the free energy for a graphene - metal system with  $\mu = m = 0$  to the ideal metal - ideal metal free energy at  $T = 300\text{K}$ .

an independent parameter for the moment, calculate the sum over  $n$  and then integrate back over  $H$  (the integration constant is fixed as zero at  $H \rightarrow \infty$ ). Thus one obtains

$$\Delta\mathcal{F}_{\text{TM}} = -\frac{T\alpha N}{8a^2} \int_H^{+\infty} dt \frac{\exp(t)(\exp(t)+1)t^2}{(\exp(t)-1)^3(8H+\pi\alpha Nt)} \quad (42)$$

At large separations one can further approximate  $8H + \pi\alpha Nt \approx 8H$  (i.e. expand in powers of  $\alpha$ ) and get

$$\Delta\mathcal{F}_{\text{TM}} \simeq -\frac{\alpha N}{128\pi a^3} \left( -\ln(1 - \exp(-H)) + \frac{H \exp(-H)}{(1 - \exp(-H))} + \frac{H^2 \exp(-H)}{2(1 - \exp(-H))^2} \right) + O(\alpha^2). \quad (43)$$

The formula (43) provides an accurate description of (42) for  $H \gtrsim 1$  where  $\Delta\mathcal{F}_{\text{TM}}$  constitutes less than 6% of the whole answer. At  $T = 300\text{K}$  this condition corresponds to distances greater than 600 nm. For smaller separations it is convenient to use (42) directly.

The TE part of the nonzero Matsubara terms of the Lifshitz formula with the coefficients  $r_{TE}^{(1)} = r_{TE}^{T=0}$  from (40) and  $r_{TE}^{(2)} = -1$  gives the following contribution in the leading order in  $\alpha$

$$\Delta\mathcal{F}_{\text{TE}} \simeq -\frac{T^2\pi\alpha N}{8} \sum_{n=1}^{+\infty} n \int_{\omega_n}^{+\infty} ds_1 \exp(-2as_1) = -\frac{T^2\pi\alpha N}{16a} \frac{\exp(-H)}{(1 - \exp(-H))^2}. \quad (44)$$

Thus, the complete result for the sum of nonzero Matsubara TM and TE terms in the approximation described above is given by (42) and (44)

$$\Delta\mathcal{F} = \Delta\mathcal{F}_{\text{TM}} + \Delta\mathcal{F}_{\text{TE}}. \quad (45)$$

Consequently, the leading  $v_F = 0$  contribution to the free energy is the sum of (36) and (45):  $\mathcal{F}_{\text{OTM}}^{(0)} + \Delta\mathcal{F}$ . It can be used for the comparison of the theory and experiment almost at all separations. As our numerical analysis shows,

a difference between the exact Lifshitz result  $\mathcal{F}$  (27) (with  $v_F = 1/300$ ,  $m = \mu = 0$ ) and considered approximation  $\mathcal{F}_{0\text{TM}}^{(0)} + \Delta\mathcal{F}$  is less than 1% for all separations between 1 and 2000 nm at the temperature  $T = 300\text{K}$ , which approximately corresponds to  $3.3 \gtrsim H \gtrsim v_F/2 = 1/600$ .

In our opinion, the distances corresponding to  $H \gtrsim v_F$  (i.e. above  $\sim 2$  nm for  $T = 300\text{K}$ ) are most relevant for a possible experiment, and the analytical expressions (42) and (44) are obtained to describe this particular regime. However, numerical studies reveal that  $\Delta\mathcal{F}_{TM,E}$  are smooth in the vicinity of  $H = 0$  point, and collate with  $T = 0$  result obtained in [9]. Indeed, from (42) and (44) one gets in this limit

$$\Delta\mathcal{F}|_{H \rightarrow 0} = -\frac{\alpha N}{128\pi a^3} \ln(1 + 8/(\alpha N\pi)) - \frac{\alpha N}{256\pi a^3}. \quad (46)$$

where the non analyticity in  $\alpha$  comes from the TM mode, and explains the precautions we took avoiding to expand the reflection coefficient in (39). Since for  $T \rightarrow 0$  the zero-frequency term  $\mathcal{F}_0$  (29) vanishes, eq. (46) represents the free energy in the leading order in  $\alpha$  in the approximation when  $v_F = 0$ . The difference between (46) and the exact Lifshitz result at  $T = 0$  with  $v_F = 1/300$  is less than 1%. We also note that at  $T = 0$  the perturbative expansion in  $\alpha$  is meaningful for  $v_F \neq 0$  only, see [9].

On Fig.1 we plot the ratio  $\rho_1$  of the Lifshitz free energy  $\mathcal{F}$  (27) divided by the high temperature asymptotics  $\mathcal{F}_{0\text{TM}}^{(0)}$  (36) at  $T = 300\text{K}$  for two systems: graphene-ideal metal and ideal metal-ideal metal. From Fig.1 it is evident that the pace of approaching the asymptotic values by the free energy in the case of a graphene – ideal metal system is much higher than in the ideal metal–ideal metal one. It is explained by the particular behavior of the components of the polarization operator at nonzero frequencies

$$\Pi_{00}(\omega_n)|_{|\mathbf{p}| \rightarrow 0} \simeq \frac{\alpha \mathbf{p}^2 c_n}{T} + O(\mathbf{p}^4), \quad \Pi_{\text{tr}}(\omega_n)|_{|\mathbf{p}| \rightarrow 0} \simeq \alpha T \tilde{c}_n + O(\mathbf{p}^2), \quad n \geq 1,$$

which induce additional  $O(\alpha)$  suppression of the corresponding contributions to the free energy. Here,  $c_n, \tilde{c}_n$  are factors of the order of unity. Because of this suppression the zero frequency TM Matsubara term dominates in the temperature dependence of the Lifshitz free energy for a graphene-metal system at much shorter separations than in the case of a metal-metal system.

It is instructive to define separate regimes on the basis of the scaling behavior of the free energy, rather than on validity of various approximations. As a function of distance,  $\mathcal{F} \sim a^{-3+\delta}$ , where  $\delta = 0$  at  $T = 0$  and  $\delta = 1$  at  $T \rightarrow \infty$ . The scaling parameter  $\delta$  varies slowly, and can thus be defined through a logarithmic derivative

$$\delta = a \frac{d}{da} [\ln a^3 |\mathcal{F}|]. \quad (47)$$

Since we are interested in rough estimates, it is enough to approximate  $\mathcal{F}$  by a rational function

$$\mathcal{F} \simeq -\frac{U + aV}{16\pi a^3}, \quad (48)$$

where  $U$  can be defined by the  $T = 0$  value (46) and  $V$  is calculated through the high temperature asymptotics, (36). Namely,

$$U = \frac{\alpha N}{8} \left[ \ln \left( 1 + \frac{8}{\alpha N\pi} \right) + \frac{1}{2} \right], \quad V = T\zeta(3). \quad (49)$$

Consequently, (47) gives

$$aT = \frac{U\delta}{\zeta(3)(1-\delta)}. \quad (50)$$

We may consider the ‘‘zero temperature’’ regime as the one where  $\delta$  is close to its  $T = 0$  value, let us say  $\delta \lesssim 0.2$ , giving  $aT \lesssim 0.004$  or  $a \lesssim 30\text{nm}$  at  $T = 300\text{K}$ . The high temperature regime, on the other hand, may be defined as  $\delta \gtrsim 0.8$  corresponding to  $aT \gtrsim 0.06$ , or  $a \gtrsim 460\text{nm}$  at  $T = 300\text{K}$ . Numerically, this bound is very close to one in the original condition,  $H \gg 1$ , which is universal for any Casimir system. However, in the graphene-metal interaction, as we already discussed, the high-temperature asymptotics is already saturated at  $H \sim 1$ , see Fig. 1. This can also be seen by considering an ‘intermediate’ scaling. At distances corresponding to  $\delta = 1/2$ , where  $H \approx 2\pi\alpha \ln \alpha^{-1}/\zeta(3) \approx 0.19$  is much smaller than unity, the high temperature asymptotic value already becomes larger than zero- $T$  contribution, i.e.  $aV > U$ , and thus this point can be considered (rather formally) as a crossover between zero and high-temperature regions.

It is interesting to note that the parameter  $U$  which governs transitions between different regimes is defined by  $\alpha$  and does not depend on  $v_F$ . One should not however overestimate this fact. All our expressions are valid for small  $v_F$  only. In such a case the free energy behaves, very roughly, as a sum of the zero temperature contribution and the zeroth Matsubara term. Therefore, the crossover between different regimes is defined by the ratio of these two contributions.

On Fig.2 we plot the ratio  $\rho_2$  of the free energy of a graphene-metal system to the ideal metal-ideal metal free energy at separations below 300 nm. The temperature is chosen as  $T = 300\text{K}$ , which means that  $H = 4\pi aT$  varies on Fig.2 from zero to 0.49. We used a plasma model for gold  $\varepsilon(i\omega) = 1 + \omega_p^2/\omega^2$  with a plasma frequency  $\omega_p = 9.0\text{eV}$  in numerical calculations of the free energy for gold semispace and a parallel graphene layer, gold reflection coefficients are standard Fresnel coefficients for TM, TE modes with a dielectric permittivity  $\varepsilon(\omega)$ , see [44]. The numerical result for the free energy of gold-graphene system divided by an ideal metal - ideal metal free energy is shown by the dashed blue curve on Fig.2. Note that the behavior of the gold-graphene free energy at short separations is one power of  $a$  different from the graphene-ideal metal free energy. This is the usual change in power law when one approaches short separations and the transition from the retarded regime to a non-retarded one takes place at separations characterized by a material wavelength  $\lambda_p = 2\pi/\omega_p$ . Thus, the result for a real metal interacting with graphene is essentially different from the ideal metal - graphene result at short separations only. The red curve which corresponds to the zero Matsubara term only is almost perfectly linear. This reflects the point that, as mentioned above, the expansion of  $\mathcal{F}_{0\text{TM}}$  around the high temperature asymptotics  $\mathcal{F}_{0\text{TM}}^{(0)}$  is governed by a small parameter  $v_F^2/(\alpha N)$ , while the term  $\mathcal{F}_{0\text{TE}}$  is suppressed by a factor  $\alpha N v_F^2$ .

Physical units can be restored in our formulas following the simple rule: in the result expressed as an appropriate power of  $aT$  divided by  $a^3$ , the former product is to be replaced by  $k_B aT/(\hbar c)$ , while  $1/a^3$  is to be substituted by  $\hbar c/a^3$ .

## V. CONCLUSIONS

We have calculated finite temperature Casimir interaction between graphene and a parallel conducting plane in the framework of the Dirac model of quasiparticles in graphene. From the theoretical point of view, it is interesting to note, that we start with a fully consistent quantum field theory model at finite temperature, and that the polarization tensor (conductivity of the graphene surface) is thus temperature dependent.

At high temperature (large separations) the free energy of interaction of suspended graphene sample and a parallel metal asymptotically behaves as the one for two conducting surfaces described by the Drude model, which yields a very strong Casimir interaction, somewhat surprising for a one-atom thick system. This feature provides an excellent opportunity for the experimental studies of the temperature Casimir effect in this system at room temperature and large separations as well as for medium ones. The energy at large separations is essentially insensitive to the model which was actually used for description of the metal's conductivity. Moreover, the interaction between two graphene samples would have exactly the same high temperature asymptotics. Such behavior is induced by the specific static limit ( $\omega = 0$ ) of the graphene reflection coefficients,  $r_{\text{TM}} \simeq 1, r_{\text{TE}} \simeq 0$  given the small Fermi velocity in graphene,  $v_F \ll 1$ . In this limit they formally coincide with the reflection coefficients for the Drude model of metals.

We studied the Lifshitz free energy for graphene-metal system in detail and obtained results that can be readily used for the comparison of the theory and experiment at room temperature and various separations. For separations corresponding to  $H \equiv 4\pi aT \gtrsim v_F$ , we used the limit  $v_F = 0$  in the Lifshitz formula to evaluate the sum of nonzero Matsubara terms. The speed of quasiparticles in graphene is much slower than the speed of photons, this is the physical reason for the accuracy of the  $v_F = 0$  limit. In this limit perturbative results in the coupling constant  $\alpha$  diverge at  $T = 0$ . Perturbation theory in  $\alpha$  does not give reliable results for graphene systems where  $v_F$  is small.

Different physical regimes were separated by investigating the dependence of the free energy on the distance,  $a$ . It appeared to be close to the typical zero temperature one,  $a^{-3}$ , for  $k_B T a/(\hbar c) \lesssim 0.004$  and approaching the high energy asymptotics  $a^{-2}$  for  $k_B T a/(\hbar c) \gtrsim 0.06$ . The formal crossover between different regimes can be chosen as  $k_B T a/(\hbar c) \approx 0.015$ . It is interesting to note that the metal-graphene system arrives at the high-temperature regime much faster than the ideal metal-ideal metal system due to the  $O(\alpha)$  suppression of the TE mode and all nonzero Matsubara terms.

We have to stress that we have considered a suspended graphene sample. In such a sample the values of  $m$  and  $\mu$  are small and, as our numerical study shows, their influence on the Casimir interaction is negligible. This approximation will not be applicable to graphene on a substrate, where one should also take into account the influence of impurities and the contribution of substrate itself to the reflection coefficients. Another point of special attention which should be taken into account when comparing the theory with experiments is the fact, that exact results in complicated geometries [43, 45–48] can be essentially different from the approximations based on the Lifshitz result for two parallel plates. In any case, the state-of-the-art experimental techniques resolve the Casimir force with total error of fractions

of percent. This permits us believe that a graphene based experiment being not an easy task is still perfectly feasible.

Finally, a comparison with some previous works on the subject is in order. As mentioned before, the leading asymptotics for the free energy of a graphene-metal system at large separations (36) coincides with one of a graphene-graphene system. Thus our findings support the results of Ref.[14] where the thermal van der Waals interaction in the later system was studied. However, our prediction for characteristic distance separating zero and high-temperature regimes (as discussed below Eq. (50)) differs from that of Ref. [14]. In our case it does not depend on the Fermi velocity  $v_F$  but does depend on the fine structure constant  $\alpha$ , while in [14] it is proportional to  $v_F$  with no dependence on  $\alpha$ . There is no direct contradiction, however, since different physical systems have been studied in our works. We disagree with the paper [15], which found practically no temperature dependence of the Casimir interaction of graphene (and which therefore also contradicts [14]). Still, the estimate for the zero-temperature case given in [15] coincides with our previous calculations [9]. Finally, the separations considered in [13] are too small to allow for a comparison with our results.

### Acknowledgments

This work was supported in parts by FAPESP (I.V.F. and D.V.V.), CNPq (D.V.V.), and by the grant RNP 2.1.1/1575 (I.V.F. and V.N.M.).

- 
- [1] A. K. Geim and K. S. Novoselov, *Nature Mater.* **6**, 183 (2007); M. I. Katsnelson, *Mater. Today* **10**, 20 (2007); A. K. Geim, *Science* **324**, 1530 (2009) arXiv:0906.3799 [cond-mat.mes-hall].
  - [2] A. H. Castro Neto, F. Guinea, N. M. R. Peres, K. S. Novoselov, and A. K. Geim, *Rev. Mod. Phys.* **81**, 109 (2009).
  - [3] G. W. Semenoff, *Phys. Rev. Lett.* **53**, 2449 (1984); D. P. DiVincenzo and E. J. Mele, *Phys. Rev. B* **29**, 1685 (1984); C. L. Kane and E. J. Mele, *Phys. Rev. Lett.* **95**, 146802 (2005).
  - [4] T. W. Appelquist, M. J. Bowick, D. Karabali and L. C. R. Wijewardhana, *Phys. Rev. D* **33**, 3704 (1986).
  - [5] E. V. Gorbar, V. P. Gusynin, V. A. Miransky and I. A. Shovkovy, *Phys. Rev. B* **66**, 045108 (2002) [arXiv:cond-mat/0202422]; V. P. Gusynin and S. G. Sharapov, *Phys. Rev. B* **73**, 245411 (2006) [arXiv:cond-mat/0512157]; V.P. Gusynin, S.G. Sharapov, J.P. Carbotte, *New J. Phys.* **11** (2009) 095013, [arXiv:0908.2803v2].
  - [6] P. K. Pyatkovskiy, *J. Phys.: Condens. Matter* **21**, 025506 (2009).
  - [7] R. Nair, P. Blake, A. N. Grigorenko, K. S. Novoselov, T. J. Booth, T. Stauber, N. M. R. Peres and A. K. Geim, *Science* **320**, 1308 (2008); A. B. Kuzmenko, E. van Heumen, F. Carbone, and D. van der Marel, *Phys. Rev. Lett.* **100**, 117401 (2008).
  - [8] K.S. Novoselov, et al., *Nature* **438**, 197 (2005). Y. Zhang, et al., *Nature* **438**, 201 (2005).
  - [9] M. Bordag, I. V. Fialkovsky, D. M. Gitman and D. V. Vassilevich, *Phys. Rev. B* **80**, 245406 (2009) [arXiv:0907.3242 [hep-th]].
  - [10] G. Barton. *J.Phys.A* **38** (13), 2997 (2005).
  - [11] M. Bordag, *J. Phys. A* **39**, 6173 (2006).
  - [12] M. Bordag, B. Geyer, G. L. Klimchitskaya and V. M. Mostepanenko, *Phys. Rev. B* **74**, 205431 (2006).
  - [13] J. F. Dobson, A. White, and A. Rubio, *Phys.Rev.Lett.***96**, 073201 (2006).
  - [14] G. Gómez-Santos, *Phys.Rev.B* **80**, 245424 (2009).
  - [15] D. Drosdoff and L. M. Woods, *Casimir Forces and Graphene Sheets*, [arXiv:1007.1231 [cond-mat.mes-hall]]
  - [16] I. Brevik, S. E. Ellingsen, and K. A. Milton, *New J.Phys.* **8**, 236 (2006).
  - [17] K. A. Milton, *J.Phys.A: Math.Gen.* **37**, 209 (2004).
  - [18] P. R. Buenzli and P. A. Martin, *Europhys.Lett.* **72**, 42 (2005).
  - [19] G. Bimonte, *Phys.Rev.A* **79**, 042107 (2009).
  - [20] M.Anteza, L.P.Pitaevskii and S.Stringari, *Phys.Rev.A* **70**, 053619 (2004).
  - [21] M.Anteza, L.P.Pitaevskii and S.Stringari, *Phys.Rev.Lett.* **95**, 113202 (2005).
  - [22] M. Boström and B.E. Sernelius, *Phys. Rev. Lett.* **84**, 4757 (2000).
  - [23] J. S. Hoye, I. Brevik, J. B. Aarseth, and K. A. Milton, *Phys.Rev.E* **67**, 056116 (2003).
  - [24] C. Genet, A. Lambrecht and S. Reynaud, *Phys.Rev.A* **62**, 012110 (2000).
  - [25] G. L. Klimchitskaya and V. M. Mostepanenko, *Phys.Rev.A* **63**, 062108 (2001).
  - [26] I. Brevik, J. B. Aarseth, J. S. Hoye, and K. A. Milton, *Phys.Rev.E* **71**, 056101 (2005).
  - [27] B. E. Sernelius, *J.Phys.A* **39**, 6471 (2006).
  - [28] L. P. Pitaevskii, *Phys.Rev.Lett.* **101**, 163202 (2008).
  - [29] D. A. R. Dalvit and S. K. Lamoreaux, *Phys.Rev.Lett.* **101**, 163203 (2008).
  - [30] V. B. Svetovoy, *Phys.Rev.Lett.* **101**, 163603 (2008).
  - [31] R. S. Decca, D. López, E. Fischbach, G. L. Klimchitskaya, D. E. Krause, and V. M. Mostepanenko, *Ann.Phys. (N.Y.)* **318**, 37 (2005) ; *Phys.Rev.D* **75**, 077101 (2007).

- [32] W. J. Kim, A. O. Sushkov, D. A. R. Dalvit and S. K. Lamoreaux, Phys. Rev. A **81**, 022505 (2010); A. O. Sushkov, W. J. Kim, D. A. R. Dalvit and S. K. Lamoreaux, *Observation of the thermal Casimir force*, arXiv: 1011.5219.
- [33] D. V. Khveshchenko, Phys. Rev. Lett. **87**, 206401 (2001).
- [34] N. Dorey, N.E. Mavromatos Nuclear Physics B **386** , 614 (1992).
- [35] Wei Li and Guo-Zhu Liu, Phys. Rev. D **81**, 045006 (2010).
- [36] V. Zeitlin, Phys. Lett. B **352** (1995) 422-427.
- [37] I. V. Fialkovsky, D.V. Vassilevich, J. Phys. A: Math. Theor. **42** (2009) 442001, arXiv: 0902.2570 [hep-th]
- [38] N.P. Landsman and Ch.G. van Weert, Physics Reports 145, Nos. 3 & 4 (1987) 141-249.
- [39] E. M. Lifshitz, Zh. Eksp. Teor. Fiz. **29**, 94 (1955) [Sov. Phys. JETP **2**, 73, (1956)]; E. M. Lifshitz and L. P. Pitaevskii, Statistical Physics, part 2 (Pergamon Press, Oxford, 1980).
- [40] E.I.Kats, Zh.Eksp.Teor.Fiz. **73**, 212 (1977) (Sov.Phys.JETP **46**, 109 (1977)).
- [41] M. T. Jaekel and S. Reynaud. Journal De Physique I, **1** (10), 1395 (1991).
- [42] M. Bordag. J. Phys. A **28**, 755 (1995).
- [43] A. Lambrecht and V. N. Marachevsky, Phys.Rev.Lett. **101**, 160403 (2008); Int.J.Mod.Phys. A **24**, 1789 (2009).
- [44] L.D.Landau, E.M.Lifshitz and L.P.Pitaevskii, Electrodynamics of Continuous Media (Pergamon Press, Oxford, 1984).
- [45] V.N.Marachevsky, Phys.Rev.D **75**, 085019 (2007); J.Phys.A **41**, 164007 (2008).
- [46] H.-C. Chiu, G. L. Klimchitskaya, V. N. Marachevsky, V. M. Mostepanenko, and U. Mohideen, Phys.Rev.B **80**, 121402(R) (2009); Phys.Rev.B **81**, 115417 (2010).
- [47] P. S. Davids, F. Intravaia, F. S. S. Rosa, D. A. R. Dalvit, Phys. Rev. A **82**, 062111 (2010).
- [48] M. Bordag and I. Pirozhenko, Phys. Rev. D **81**, 085023 (2010).